

Synthesis, Characterization and Crystal Structures of Technetium(V)–Oxo Complexes Useful in Nuclear Medicine. 1. Complexes of Mercaptoacetylglucylglycylglycine (MAG₃) and Its Methyl Ester Derivative (MAG₃OMe)

Glenn Grummon, Raghavan Rajagopalan, Gus J. Palenik,¹ Anna E. Koziol,¹ and Dennis L. Nosco*

Mallinckrodt Medical, Inc., 675 McDonnell Blvd, St. Louis, Missouri 63134

Received July 7, 1994[Ⓢ]

The technetium(V) complex $[^{99g}\text{TcO}(\text{MAG}_3)]^-$ (MAG₃ = mercaptoacetylglucylglycylglycine) can be prepared by substitution of the free ligand onto $[^{99g}\text{TcOCl}_4]^-$. The product is characterized by UV–visible spectroscopy, FAB mass spectrometry, ¹H and ¹³C NMR spectroscopy, and X-ray crystallography. $(\text{Ph}_4\text{As})[^{99g}\text{TcO}(\text{MAG}_3)]^-$, chemical formula $\text{TcAsSO}_6\text{N}_3\text{C}_{32}\text{H}_{29}$, crystallizes in the monoclinic space group $P2_1/n$ with $Z = 4$ and lattice parameters $a = 12.252(6)$ Å, $b = 10.169(6)$ Å, $c = 24.579(7)$ Å, $\beta = 92.04(3)^\circ$, and $V = 3060(2)$ Å³. The final R value is 0.042. The technetium coordination geometry is square pyramidal with $\text{Tc}=\text{O} = 1.647(3)$ Å, $\text{Tc}-\text{S} = 2.279(2)$ Å, and $\text{Tc}-\text{N} = 1.987(15)$ Å on average. The MAG₃ ligand is usually prepared in a form wherein the thiol functionality is protected by a benzoyl group. Preparation of the $[^{99m}\text{TcO}(\text{MAG}_3)]^-$ renal function imaging radiopharmaceutical by the Sn(II) reduction of $[^{99m}\text{TcO}_4]^-$ in the presence of benzoyl–MAG₃ is also described. HPLC comparisons verify that the two products $[^{99g}\text{TcO}(\text{MAG}_3)]^-$ and $[^{99m}\text{TcO}(\text{MAG}_3)]^-$ are chemically identical. The methyl ester derivative of MAG₃ forms a stable complex with the TcO^{3+} core and $[^{99g}\text{TcO}(\text{MAG}_3\text{OMe})]^-$ is shown by HPLC to be a side product generated during the formation of $[^{99g}\text{TcO}(\text{MAG}_3)]^-$. $[^{99g}\text{TcO}(\text{MAG}_3\text{OMe})]^-$ is characterized herein by its direct synthesis and structural characterization. Two different conformations of the ligand in $(\text{PPh}_4)[^{99g}\text{TcO}(\text{MAG}_3\text{OMe})]\cdot 2\text{H}_2\text{O}$ have been shown crystallographically: polymorph 1 crystallizes in the space group $P\bar{1}$ with lattice constants $a = 11.054(4)$ Å, $b = 12.583(5)$ Å, $c = 13.810(5)$ Å, $\alpha = 68.79(3)^\circ$, $\beta = 76.15(3)^\circ$, $\gamma = 88.86(3)^\circ$, $V = 1734(1)$ Å³, and $Z = 2$; polymorph 2 crystallizes in $P\bar{1}$ with lattice constants $a = 12.62(1)$ Å, $b = 12.87(2)$ Å, $c = 13.09(2)$ Å, $\alpha = 117.5(1)^\circ$, $\beta = 111.19(9)^\circ$, $\gamma = 90.3(1)^\circ$, $V = 1719(4)$ Å³, and $Z = 2$. Averaged bond lengths for $[^{99g}\text{TcO}(\text{MAG}_3\text{OMe})]^-$ are $\text{Tc}=\text{O} = 1.656(3)$ Å, $\text{Tc}-\text{S} = 2.289(3)$ Å, and $\text{Tc}-\text{N} = 2.00(3)$ Å. The geometry about technetium is square pyramidal with insignificant chemical differences between the two polymorphs. The syntheses of the ligands MAG₃ and MAG₃OMe are described.

Introduction

Until recently, the radiopharmaceutical routinely used for the evaluation of kidney function was ¹³¹I-labeled *o*-iodohippurate (Hippuran R). The unfavorable characteristics of the isotope ¹³¹I (long half-life of 8 days, high γ energy of 364 KeV, β^- emission) resulted in high radiation doses to the patient, so ¹²³I-labeled hippurate was considered as an alternative. However, the advantages of shipping the long half-life ¹³¹I product without significant loss of potency were lost upon switching to the shorter half-life ¹²³I ($t_{1/2} = 13$ h). The clear advantages of ^{99m}Tc as an isotope for imaging are well-known² and much effort was expended to develop ^{99m}Tc replacements for the iodinated hippurate agents. Early experimental complexes such as ^{99m}Tc–dimercaptosuccinic acid (Tc–DMSA) and ^{99m}Tc–diethylenetriaminepentaacetic acid (Tc–DTPA) showed some promise.³ Research on ^{99m}Tc complexes of amino acid derivatives by Fritzberg and co-workers led to the 1986 discovery of ^{99m}Tc–oxomercaptoacetyltriglycine (abbreviated ^{99m}Tc–MAG₃

in the medical literature, abbreviated $[^{99m}\text{TcO}(\text{MAG}_3)]^-$ here) as a potential replacement for the iodinated hippurates.⁴ The agent $[^{99m}\text{TcO}(\text{MAG}_3)]^-$ has since gained acceptance as the gold standard for renal function imaging.^{5,6} This paper establishes the structure of this radiopharmaceutical by direct synthesis and characterization of the analogous ^{99g}Tc complex. Also described are the characterizations of some important byproducts of the $[^{99g}\text{TcO}(\text{MAG}_3)]^-$ synthesis.

Experimental Section

Caution! ^{99g}Tc emits a low energy (0.292 MeV) β particle with a half-life of 2.12×10^5 yr. When handled in milligram amounts, ^{99g}Tc does not present a serious health hazard since common laboratory

* Abstract published in *Advance ACS Abstracts*, February 15, 1995.

- Present address: Department of Chemistry, University of Florida, Gainesville, FL 32611.
- Deutsch, E.; Libson, K.; Jurisson, S.; Lindoy, L. F. *Prog. Inorg. Chem.* **1983**, *30*, 75–139. Deutsch, E.; Libson, K. *Comments Inorg. Chem.* **1984**, *3*, 83–103. Clarke, M. J.; Podbielski, L. *Coord. Chem. Rev.* **1987**, *78*, 253–331.
- Fraile, M.; Castell, J.; Buxeda, M.; Cuartero, A.; Cantarell, C.; Domenech-Torné, F. M. *Eur. J. Nucl. Med.* **1989**, *15*, 776–779. Russell, C. D.; Dubovsky, E. V. *J. Nucl. Med.* **1989**, *30*, 2053–2057. Blafox, M. D. *J. Nucl. Med.* **1991**, *32*, 1301–1309. See also ref 5 for more clinical comparisons of radiopharmaceutical agents.

(4) Fritzberg, A. R.; Kasina, S.; Eshima, D.; Johnson, D. L. *J. Nucl. Med.* **1986**, *27*, 111–116.

(5) Verbruggen, A. M. *Eur. J. Nucl. Med.* **1990**, *7*, 346–364. Bubeck, B.; Brandau, W.; Weber, E.; Kälble, T.; Parekh, N.; Georgi, P. *J. Nucl. Med.* **1990**, *31*, 1285–1293. Eshima, D.; Fritzberg, A. R.; Taylor, A. *Semin. Nucl. Med.* **1990**, *20*, 28–40. Hvid-Jacobsen, K.; Thomsen, H. S.; Nielsen, S. L. *Acta Radiol.* **1990**, *31*, 83–86. Russell, C. D.; Thorstad, B. L.; Yester, M. V.; Stutzman, M.; Dubovsky, E. V. *J. Nucl. Med.* **1988**, *29*, 1931–1933. Al-Nahhas, A. A.; Jafri, R. A.; Britton, K. E.; Solanki, K.; Bomanji, J.; Mather, S.; Carroll, M. A.; Al-Janabi, M.; Frusciant, V.; Ajdinowic, B.; Fiore, F.; Demena, S.; Nimmon, C. C. *Eur. J. Nucl. Med.* **1988**, *14*, 453–462. Taylor, A.; Eshima, D. *J. Nucl. Med.* **1988**, *29*, 616–622. Taylor, A.; Eshima, D.; Christian, P. E.; Milton, W. *Radiology* **1987**, *162*, 365–370. Taylor, A.; Eshima, D.; Alazraki, N. *Eur. J. Nucl. Med.* **1987**, *12*, 510–514.

(6) FDA approval for $[^{99m}\text{TcO}(\text{MAG}_3)]^-$ in the USA was granted in 1990. This agent is supplied by Mallinckrodt, Medical, Inc., under the tradename Technescan MAG₃.

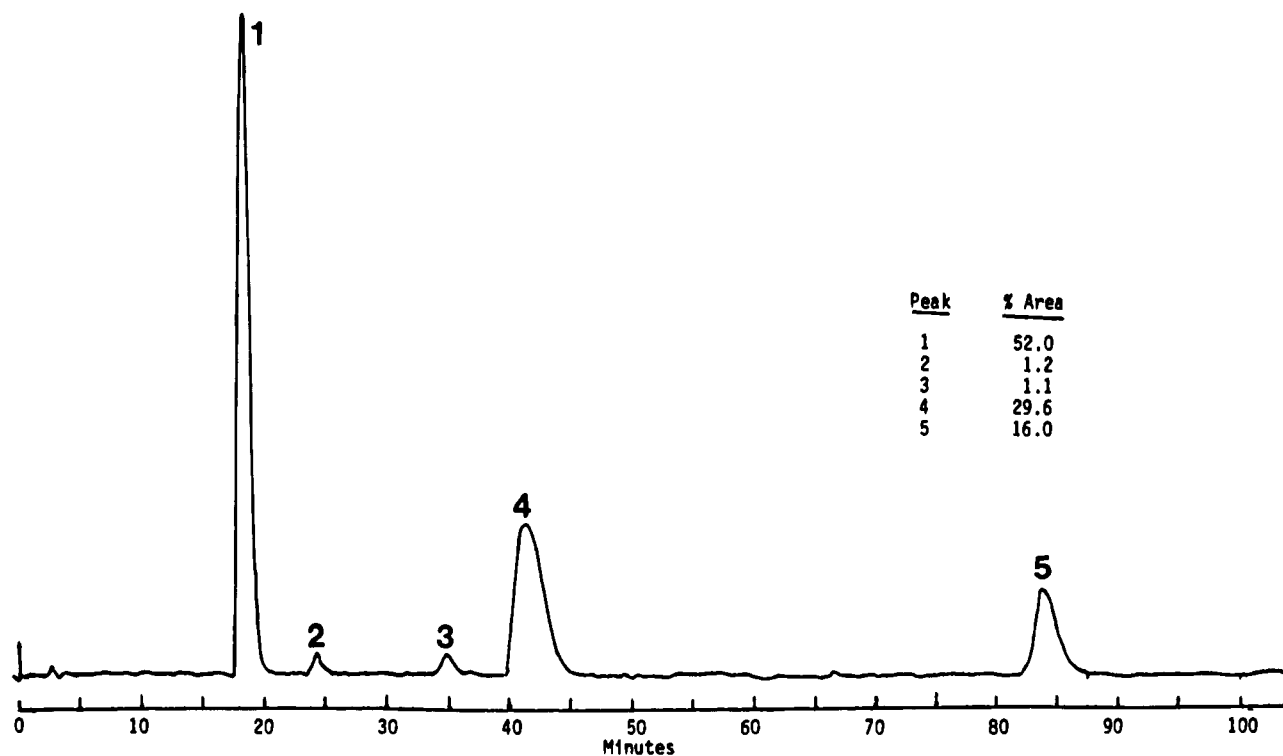


Figure 1. HPLC trace (UV detection, ion-pairing mode) of the reaction mixture from the preparation of $[^{99\text{Tc}}\text{O}(\text{MAG}_3)]^-$. Peak 1 represents $[^{99\text{Tc}}\text{O}(\text{MAG}_3)]^-$ while peak 5 represents $[^{99\text{Tc}}\text{O}(\text{MAG}_3\text{OMe})]^-$. Peak 4 is discussed in the text.

Table 1. Crystallographic Data for $[\text{AsPh}_4][^{99\text{Tc}}\text{O}(\text{MAG}_3)]$ (6), $[\text{PPh}_4][^{99\text{Tc}}\text{O}(\text{MAG}_3\text{OMe})]\cdot 2\text{H}_2\text{O}$ (7), and $[\text{PPh}_4][^{99\text{Tc}}\text{O}(\text{MAG}_3\text{OMe})]\cdot 2\text{H}_2\text{O}$ (Second Polymorph) (8)

	6	7	8
formula	$\text{TcAsSO}_6\text{N}_3\text{C}_{32}\text{H}_{29}$	$\text{TcSPO}_8\text{N}_3\text{C}_{33}\text{H}_{35}$	$\text{TcSPO}_8\text{N}_3\text{C}_{33}\text{H}_{35}$
fw	757.49	763.60	763.60
λ , Å	0.710 73	0.710 73	0.710 73
space group	$P2_1/n$	$P1$	$P1$
a , Å	12.252(6)	11.054(4)	12.622(14)
b , Å	10.169(6)	12.583(5)	12.867(19)
c , Å	24.579(7)	13.810(5)	13.085(19)
α , deg		68.79(3)	117.47(11)
β , deg	92.04(3)	76.15(3)	111.19(9)
γ , deg		88.86(3)	90.34(11)
V , Å ³	3060(2)	1734(1)	1719(4)
Z	4	2	2
T , °C	25	25	25
ρ (calc), g cm ⁻³	1.644	1.463	1.475
μ , cm ⁻¹	16.42	5.58	5.63
R^a	0.042	0.038	0.052
R_w^a	0.030	0.032	0.035

$$^a R = (\sum|\Delta F|)/\sum|F_o|; R_w = [(\sum w|\Delta F|^2)/\sum wF_o^2]^{1/2}.$$

materials provide adequate shielding. However, normal radiation safety procedures must be used at all times, especially when dealing with solid samples, to prevent contamination and inadvertent inhalation. The metastable isotope $^{99\text{m}}\text{Tc}$ decays by γ emission (141 KeV) with a half-life of 6 h and should be handled only in a controlled environment by qualified personnel trained in radiation safety precautions.

Reagents and Measurements. Unless otherwise noted, all chemicals were of reagent grade and were used as received from the manufacturer. Technetium in the form $\text{Na}^{99\text{Tc}}\text{O}_4$ was obtained from Oak Ridge National Laboratory. All laboratory reagents were purchased from Aldrich Chemical Co. ^1H and ^{13}C NMR spectra were obtained on a JEOL FX90Q instrument operating at 90 MHz. Ion-paired high pressure liquid chromatography (HPLC) was performed using a Waters HPLC system on a 10 μm , 250 \times 4.6 mm (or 200 \times 25 mm) C18 column (Waters Novapak) eluted with 20% ethanol/80% water and 0.005 M *tert*-butylammonium phosphate at pH 6.3 as the

mobile phase. Standard reverse phase HPLC was performed using a C18 column (Alltech 250 \times 4.6 mm) and a gradient system with solvent A composed of 0.01 M sodium phosphate in water and solvent B composed of 5% ethanol/95% water and 0.01 M sodium phosphate at pH 6.3. The following gradient was used: 0–5 min, 100% solvent A; for 5–35 min, a linear gradient to 100% solvent B; then from 35–45 min the column was eluted with 100% solvent B. Thin-layer chromatography (TLC) plates were obtained from Whatman (C18) and used with a 60/40/1 water/methanol/acetic acid as elution phase. UV–visible spectra were recorded on a Beckman DU-40 spectrophotometer. Extinction coefficients were calculated on a per mole $^{99\text{Tc}}$ basis using the observed UV–vis absorbances of recrystallized $\text{NH}_4^{99\text{Tc}}\text{O}_4$ and concentrations from β^- counting measurements on a Beckman LS 3801 scintillation counter. Standard curves of $^{99\text{Tc}}$ concentration vs counts were generated on the same instrument. Low resolution fast atom bombardment (FAB) mass spectrometry experiments were performed commercially by Shrader Laboratories, Detroit, MI, on a VG ZAB-SE double focusing spectrometer using a “magic bullet” matrix (3:1 dithiothreitol/dithioerythritol). Both positive and negative ion spectra were obtained. Xenon was used as the primary beam gas, and the ion gun was operated at 8 KV. Data were collected at 15 s/10 units of mass. Accurate masses of the quasimolecular ions were measured using the matrix ion at m/z 369.19719 as a reference.

All single crystal X-ray diffraction experiments were performed on a Nicolet R3m automated diffractometer with a graphite monochromator and $\text{MoK}\alpha$ radiation. Crystallographic data are summarized in Table 1. No corrections for absorption or extinction were made. Structure solutions and refinements used the programs of *SHELXTL*.^{7a} Neutral atom scattering factors and corrections for anomalous dispersion were from ref 7b.

Synthesis of *S*-Benzoylmercaptoacetic Acid (1). Mercaptoacetic acid (269 g) and triethylamine (590 g) were dissolved in 2 L of an acetonitrile/water solution (1:1 v/v). The solution was stirred and cooled to 10 °C. Benzoyl chloride (410 g) was added and the preparation proceeded analogously to that described by Brandau *et al.*⁸ Recrys-

(7) (a) Sheldrick, G. M. *Desktop SHELXTL*, Nicolet X-ray Instruments: Madison, WI, 1986. (b) *International Tables for X-ray Crystallography*; Kynoch Press: Birmingham, England, 1974.

(8) Brandau, W.; Bubeck, B.; Eisenhut, M.; Taylor, D. M. *Appl. Radiat. Isot.* **1988**, *39*, 121–129.

tallization from ethyl acetate/hexane yielded colorless needles (260 g from the first crop; an additional 50 g from the mother liquor). Yield 54%, mp 104–106 °C (lit. mp 104–105⁸ and 102–103 °C⁹). Carbon and proton NMR spectra were consistent with the structure.⁸ Anal. Calcd for C₉H₈O₃S: C, 55.09; H, 4.11; S, 16.34. Found: C, 55.28; H, 4.22; S, 16.33.

Synthesis of *N*-(*S*-Benzoylmercapto)acetoxysuccinimide (2). A stirred mixture of *N*-hydroxysuccinimide (117 g) and *S*-benzoylmercaptoacetic acid (196 g) in dry acetone (1.2 L) was treated with a solution of dicyclohexylcarbodiimide (210 g) in acetone (800 mL). The heterogeneous mixture was stirred at ambient temperature for 16 h. It was then filtered to remove dicyclohexylurea, and the filtrate was evaporated to dryness at reduced pressure. Ether (1 L) was added, and the crude product was collected and dried. Recrystallization from acetone/hexane gave colorless needles, mp 138–140 °C (lit. mp 135–137 °C^{8,9}). Yield: 159 g (54%). Carbon and proton NMR spectra were consistent with the formulation.⁸ Anal. Calcd for C₁₃H₁₁NO₅S: C, 53.24; H, 3.78; N, 4.78; S, 10.93. Found: C, 53.35; H, 4.00; N, 4.66; S, 11.01.

Synthesis of *N*-(*S*-Benzoylmercapto)acetylglcylglycylglycine, (3), (Benzoyl-MAG₃). *N*-(*S*-Benzoylmercapto)acetoxysuccinimide (29.3 g) in 150 mL of acetonitrile was heated gently and stirred until all the solid dissolved. A solution of triglycine (18.9 g) in a 1.03 N NaOH solution (96 mL) was added, and the reaction mixture was stirred at ambient temperature for 3 h. (Note that initially the solution became turbid and some precipitate formed. The reaction mixture, however, became clear within 10 min.) The mixture was diluted with water (50 mL) and treated with concentrated HCl (12 mL). The mixture was refrigerated (~4 °C) for 4 h, after which the precipitate was collected, washed with water, and dried. The crude product (34 g) was suspended in water (500 mL), heated to 60–65 °C, and then treated with hot acetone to dissolve the solid. The clear solution was allowed to cool slowly over 16 h resulting in colorless crystals. Yield: 30 g (82%), mp 203–204 °C (lit. mp 193–195⁸ and 195–196 °C⁴). The carbon NMR spectrum was consistent with the structure.⁸ Anal. Calcd for C₁₅H₁₇N₃O₆S: C, 49.02; H, 4.66; N, 11.44; S, 8.73. Found: C, 48.79; H, 4.57; N, 11.07; S, 8.97.

Synthesis of *N*-(*S*-Benzoylmercapto)acetylglcylglycylglycine Methyl Ester, (4), (Benzoyl-MAG₃OMe). A mixture of *N*-(*S*-benzoylmercapto)acetylglcylglycylglycine (36.7 g), *N*-hydroxysuccinimide (12.1 g), and dicyclohexylcarbodiimide (21.6 g) in anhydrous dimethylformamide (300 mL) was stirred at ambient temperature for 36 h. The reaction mixture was diluted with acetone (300 mL) and cooled to 0 °C in an ice bath for 1 h. The mixture was then filtered to remove dicyclohexylurea and the filtrate was poured into a stirring solution of ether (4 L). The resulting precipitate was collected by filtration, washed with ether, and dried. The solid was then dissolved in hot methanol (300 mL) and allowed to cool to ambient temperature overnight. The resulting light pink crystals were collected by filtration, washed with ice-cold methanol, and dried. Yield: 31.5 g (82.7%), mp 204–205 °C. Anal. Calcd for C₁₆H₁₉N₃O₆S·0.1H₂O: C, 50.15; H, 5.05; N, 10.97; S, 8.35. Found: C, 49.82; H, 5.09; N, 11.15; S, 8.36.

Syntheses of Na[^{99m}TcO(MAG₃)] (5), (Ph₄As)[^{99m}TcO(MAG₃)] (6), and (Ph₄P)[^{99m}TcO(MAG₃OMe)] (7,8). A 4.2 mL sample of an aqueous 0.67 M Na^{99m}TcO₄ solution (0.52 g, 2.8 mmol of NaTcO₄) was diluted with 20 mL of 12 M HCl. This solution was allowed to stir for 10 min and then evaporated to near dryness in vacuo at <40 °C on a rotary evaporator. Then 10 mL of 12 M HCl was added and the solution taken completely to dryness to yield a yellow-green solid which was dissolved in 25 mL methanol and filtered. The resulting olive-green solution of [^{99m}TcOCl₄]⁻ was then deaerated for 10 min with Ar and stoppered. During this time 35 mL of dried, distilled methanol was deaerated with Ar for 5 min. To the deaerated methanol was added 1.14 g benzoyl-MAG₃ (3.1 mmol), and after this dissolved, 0.143 g (6.2 mmol) of Na in 5 mL of deaerated methanol was added in one portion. This mixture was stoppered and sonicated at room temperature for 1 h in a 50–60 Hz Sonicor ultrasonic cleaning bath.

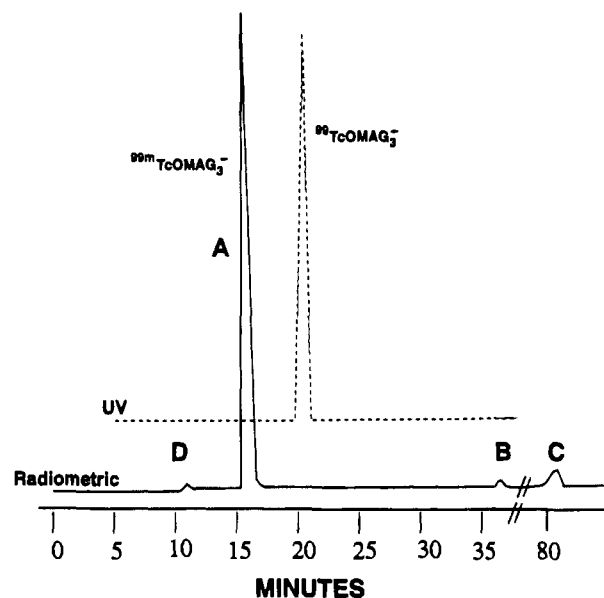


Figure 2. HPLC co-elution tracings in ion-pairing mode of the [^{99m}TcO(MAG₃)]⁻ preparative solution compared with [^{99m}TcO(MAG₃)]⁻, confirming the chemical equivalency of the two species.

The resulting solution of deprotected MAG₃ solution was then slowly added (dropwise over 5 min) under Ar to the [^{99m}TcOCl₄]⁻. The reaction solution was sonicated for 30 min and allowed to stir overnight at room temperature to yield a golden-brown solution. This was then treated with another 0.143 g of Na in 5 mL of methanol and the mixture was refluxed for 15 min. The solution was then filtered through diatomaceous earth to remove a black precipitate and the supernatant concentrated to a small volume *in vacuo* on a rotary evaporator at 40 °C. A small aliquot of this mixture (diluted in water to pH 4.4) was chromatographed on HPLC and TLC C18 plates, both of which gave three major and two minor products. An HPLC trace of this crude mixture under ion-pairing conditions is shown in Figure 1. The HPLC trace of the same mixture without addition of the ion-pairing agent produced a reversal in the relative positions of peaks 1 and 4. The entire mixture was then chromatographed on a 53 cm × 2.2 cm C18 (Whatman) column using 1:2 ethanol–water to separate the three major yellow-orange bands. HPLC analysis of these bands showed that they correspond to bands numbered 1, 4, and 5 in the HPLC of Figure 1. At this point the technetium complexes are present as Na⁺ salts. All three bands were then reduced in volume and a portion of each was treated dropwise with a solution of tetraphenylphosphonium chloride or tetraphenylarsonium chloride. Precipitates were generated from the bands labeled 1 and 5 in Figure 1. No precipitate was produced from band 4 after it was eluted from the large column, even after concentration of the tetraphenylarsonium-containing solution. The two precipitates were redissolved in ethanol and treated with water until a slight cloudiness developed at which time a small amount of ethanol was added to produce a clear solution. Slow evaporation of the resulting solution produced one type of crystal for band 1 and two types of crystals for band 5. The relative yields of products corresponding to peaks 1, 4, and 5 in Figure 1 are 52%, 30%, and 16%, respectively.

Peak 1 is confirmed to be Na[^{99m}TcO(MAG₃)] by an X-ray crystal structure analysis of the tetraphenylarsonium salt (*vide infra*). Analytical data for Na[^{99m}TcO(MAG₃)] are as follows. UV–vis (1:2 ethanol–water) [λ, nm (ε, M⁻¹cm⁻¹): 428 (161), 320 sh (2060), 270 sh (5620), 236 (9130), 204 (9510)]. FAB MS positive ion spectra contain MH, MNa, and MNa₂ ions. Negative ion spectra contain M–H ions. Exact mass (*m/e*, positive ion mode): MH⁺(obsd) = 375.943 confirming the composition C₈H₁₀N₃O₆STc. Analytical data for (AsPh₄)[^{99m}TcO(MAG₃)] are as follows. ¹H NMR (DMSO-*d*₆, ppm): 7.7–8.0 (m, 20 H from AsPh₄); 4.53, 4.41 (d,d, 2H, NCH₂, *J* = 16 Hz); 4.37, 4.18 (d,d, 2H, NCH₂, *J* = 16 Hz); 4.04 (s, 2H, NCH₂COOH); 3.85, 3.57 (d,d, 2H, SCH₂, *J* = 16 Hz). ¹³C NMR (DMSO-*d*₆, ppm): 186.3, 186.2, 183.9 (NC=O); 172.5 (COOH); 116–136 (PPh₄); 56.4, 53.7, 53.6, 36.8 (CH₂).

(9) Schneider, R. F.; Subramanian, G.; Feld, T. A.; McAfee, J. G.; Zapf-Longo, C.; Palladino, E.; Thomas, F. D. *J. Nucl. Med.* **1984**, *25*, 223–229.

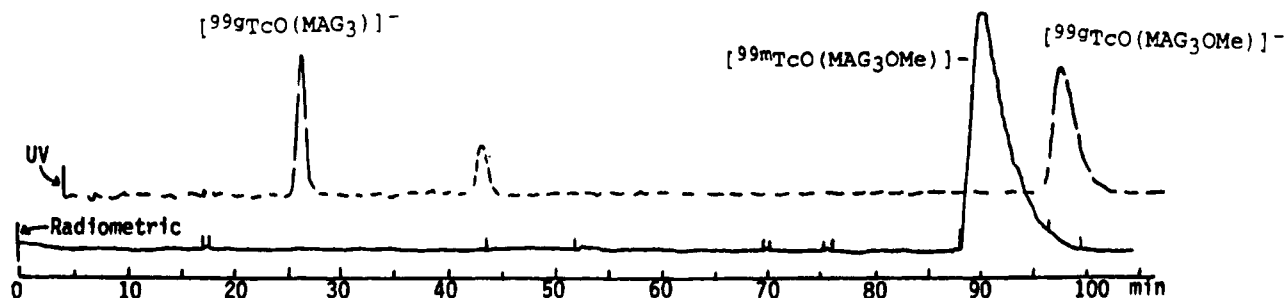
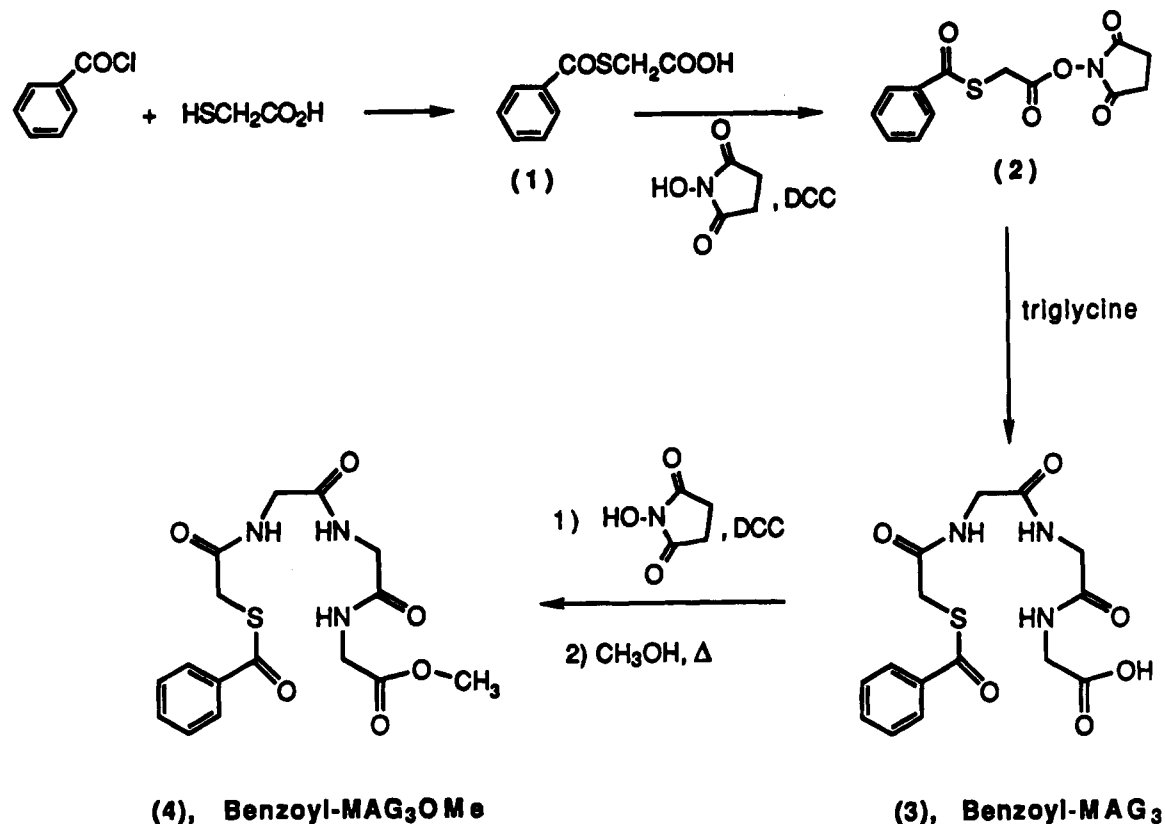


Figure 3. Overlay of HPLC tracings in ion-pairing mode under identical conditions of the reaction mixtures from the preparation of $[^{99g}\text{TcO}(\text{MAG}_3)]^-$ (---) compared to that of $[^{99m}\text{TcO}(\text{MAG}_3\text{OMe})]^-$ (—).

Scheme 1



Peak 5 is identified as $\text{Na}[^{99g}\text{TcO}(\text{MAG}_3\text{OMe})]$ by X-ray crystal structure analyses of the two crystalline forms of the tetraphenylphosphonium salts. Analytical data for $\text{Na}[^{99g}\text{TcO}(\text{MAG}_3\text{OMe})]$ are as follows. UV-vis (1:2 ethanol:water) [λ , nm (ϵ , $\text{M}^{-1}\text{cm}^{-1}$): 428 (183), 324 sh (2210), 267 sh (6370), 233 (13 300), 204 (11 400)]. FAB MS positive ion spectra contain MH, MNa, and MNa₂ ions. Negative ion spectra contain M-H ions. Exact mass (*m/e*, positive ion mode): MH⁺ (obsd) = 389.958 confirming the composition C₉H₁₂N₃O₆STc.

Synthesis of $\text{Na}[^{99m}\text{TcO}(\text{MAG}_3)]$ by Sn(II) Reduction of $^{99m}\text{TcO}_4^-$. First, 400 mg of sodium tartrate dihydrate was dissolved in 10 mL of distilled water which was adjusted to pH 8 with 0.1 M NaOH. Then, 10 mg of benzoyl-MAG₃ was dissolved into this solution by sonication. The resulting solution was deaerated with Ar for 10 min, and 1 mL of a SnCl₂ solution (0.2 g SnCl₂·H₂O in 2 mL of 12 M HCl added to 100 mL of deaerated water) was added. Then 1 mL of this mixture was added to 3 mL of $^{99m}\text{TcO}_4^-$ in saline (eluted from a Mallinckrodt Mo/Tc generator) and the reaction vial sealed and heated at 100 °C for 10 min. The yield in this procedure is usually >95% $[^{99m}\text{TcO}(\text{MAG}_3)]^-$. The identity of the product was confirmed by HPLC comparisons with known $[^{99g}\text{TcO}(\text{MAG}_3)]^-$, illustrated in Figure 2.

The nature of peak B in Figure 2 was investigated by observing its decomposition with time. The material was first isolated chromatographically under non-ion-paired HPLC conditions in 0.01 M aqueous phosphate buffer at pH 6.3. The solution was periodically sampled and submitted for ion-paired HPLC, because peak separation is greater

under ion-paired conditions. Within 24 h, complete conversion of this material to $[^{99m}\text{TcO}(\text{MAG}_3)]^-$ was demonstrated (Figure B, supplementary material).

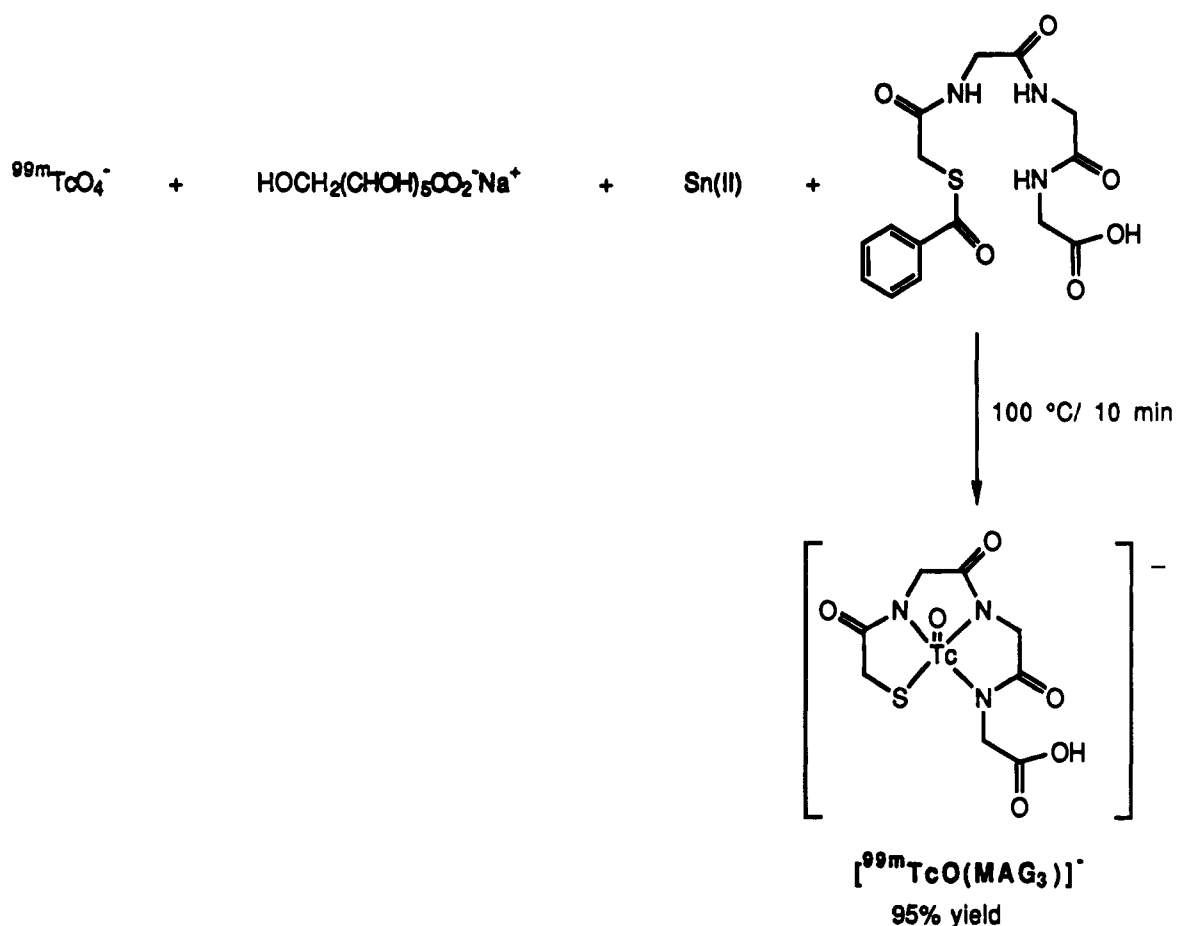
Synthesis of $\text{Na}[^{99m}\text{TcO}(\text{MAG}_3\text{OMe})]$. This preparation is analogous to that for $\text{Na}[^{99m}\text{TcO}(\text{MAG}_3)]$ given above, except that the ligand used was benzoyl-MAG₃OMe. The overall yield was 98%. Figure 3 shows the HPLC of $[^{99m}\text{TcO}(\text{MAG}_3\text{OMe})]^-$ compared with that of a mixture of $[^{99g}\text{TcO}(\text{MAG}_3\text{OMe})]^-$ and $[^{99g}\text{TcO}(\text{MAG}_3)]^-$. This comparison confirms the identity of $[^{99m}\text{TcO}(\text{MAG}_3\text{OMe})]^-$.

Results

Syntheses. The synthesis of the benzoyl-protected precursor of the ligand MAG₃ (3) is diagrammed in Scheme 1. The methyl ester ligand (4) is prepared in a two-step, one-pot procedure from (3) through activation of the carboxyl group of (3) followed by methanolysis of the corresponding active ester.

The reaction of $[^{99m}\text{TcO}_4]^-$ with benzoyl-MAG₃ to yield the renal function imaging agent $[^{99m}\text{TcO}(\text{MAG}_3)]^-$ proceeds through reaction Scheme 2. This scheme is the same as that employed in commercial radiopharmaceutical kits, except that the reactant amounts given in the Experimental Section are

Scheme 2



slightly different. The preparation detailed herein results in a product of $\geq 95\%$ radiochemical purity.

Early preparations of $[\text{MAG}_3\text{TcO}]^-$ utilized nonoptimized preparations of the ligand MAG_3 , with the result that undesirable levels of impurities were present in the final radiotracer.^{8,10} As part of an investigation into these impurities and side-reactions, the byproducts generated during the preparation of $[\text{MAG}_3\text{TcO}]^-$ have been examined. HPLC indicated that three minor side products are generated (peaks B, C, and D in Figure 2). One of these components is highly charged and hydrophilic (peak B). This can be deduced by comparison of the HPLC elution of this peak with and without the ion-pairing agent: in ion-pairing mode the complex elutes at ~ 37 min; in standard reverse phase it elutes at ~ 12 min (Figure A, supplementary material). With time, this hydrophilic material changes to $[\text{MAG}_3\text{TcO}]^-$; the conversion of this chromatographically purified side product to $[\text{MAG}_3\text{TcO}]^-$ is illustrated in Figure B. The second significant impurity (peak C) in the $[\text{MAG}_3\text{TcO}]^-$ preparation, which only occurs when using benzoyl- MAG_3 prepared by old synthetic routes,⁴ elutes at very long retention times under both ion-pairing and non-ion-pairing conditions; this implies that the material is lipophilic in its own right, independent of charge. The third side product (peak D) is a mixture of TcO_4^- and Tc -tartrate, the two main impurities in Technescan MAG_3 .¹¹

Syntheses employing macroscopic amounts of ^{99g}Tc were conducted to obtain structural information on $[\text{MAG}_3\text{TcO}]^-$ and the side products of the ^{99m}Tc reaction. Attempts to prepare

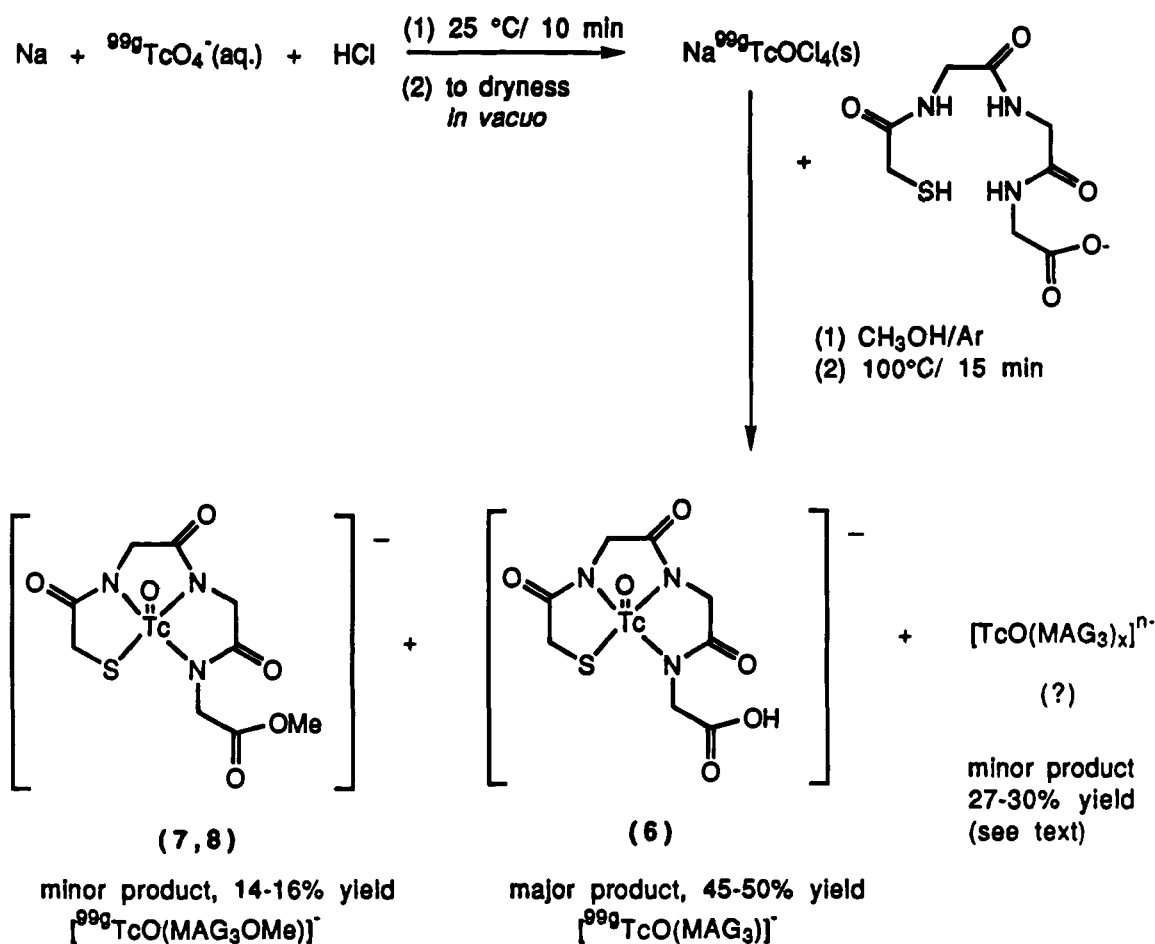
$[\text{MAG}_3\text{TcO}]^-$ by the same route used to prepare the ^{99m}Tc analog were unsuccessful. Using this route (Sn(II) reduction of pertechnetate) when free MAG_3 ligand was used instead of the protected benzoyl- MAG_3 ligand, only 5% $[\text{MAG}_3\text{TcO}]^-$ complex was produced. The synthesis of $[\text{MAG}_3\text{TcO}]^-$ that proved most successful was that which utilizes $[\text{MAG}_3\text{TcOCl}_4]^-$ as starting material, methanol as solvent, and free MAG_3 ligand as reactant. The yields were approximately 45–50% $[\text{MAG}_3\text{TcO}]^-$ and 41–46% soluble impurities. This reaction is outlined in Scheme 3. The HPLC analysis of the product mixture using ion-pairing conditions is shown in Figure 1. Peak 1 is identified as $[\text{MAG}_3\text{TcO}]^-$ by single crystal X-ray analysis and is characterized by UV-vis spectroscopy, FAB MS, and ^1H and ^{13}C NMR spectroscopy. Peak 5 is identified as $[\text{MAG}_3\text{TcO}(\text{OMe})]^-$ by X-ray crystallography and analytical characterization.

Crystallography. The X-ray crystal structure analyses of three complexes are presented. All contain the isotope ^{99g}Tc . Fractional coordinates for $[\text{AsPh}_4][\text{MAG}_3\text{TcO}]^-$, (6), are given in Table 2, and the labeling and geometry of the anion are shown in Figure 4. The structure of the anion $[\text{MAG}_3\text{TcO}]^-$ is important with respect to the commercial imaging agent $[\text{MAG}_3\text{TcO}]^-$. The structure of $[\text{PPh}_4][\text{MAG}_3\text{TcO}(\text{OMe})]\cdot 2\text{H}_2\text{O}$, (7), confirms the identity of one of the impurities sometimes present in the $[\text{MAG}_3\text{TcO}]^-$ commercial preparation. A second crystalline form of $[\text{PPh}_4][\text{MAG}_3\text{TcO}(\text{OMe})]\cdot 2\text{H}_2\text{O}$, (8), was obtained from the mother liquor after two crops of crystals were harvested. This second polymorph appeared more striated than the first and gave longer rods in shape. Both polymorphs are chemically equivalent although crystallographically nonequivalent. Fractional coordinates for $[\text{PPh}_4][\text{MAG}_3\text{TcO}(\text{OMe})]\cdot 2\text{H}_2\text{O}$ can be found in

(10) Brandau, W.; Bubeck, B.; Schober, O.; Taylor, D. M. *Radionuclides Nephro-Urol.* **1990**, *79*, 11–16.

(11) Nosco, D. L.; Wolfangel, R. G.; Bushman, M. J.; Grummon, G. D.; Marmion, M. E.; Pipes, D. W. *J. Nucl. Med. Tech.* **1993**, *21*, 69–74.

Scheme 3



Tables 3 and 4 respectively for the two polymorphs. Figures 5 and 6 show the atomic labeling of the anions, which is analogous to that for $[\text{TcO}(\text{MAG}_3)]^-$ as far as possible. Bond lengths and angles for all three anions are compared in Tables 5 and 6. All atoms occupy general positions in the unit cells.

The anionic complexes exhibit square pyramidal geometry. The technetium atom lies 0.74–0.76 Å out of the N_3S basal plane toward the oxo atom. The chelate bite angles average $82.6(2)^\circ$ for $\text{S}-\text{Tc}-\text{N}$ and $78.3(3)^\circ$ for $\text{N}-\text{Tc}-\text{N}$. The structures of $[\text{TcO}(\text{MAG}_3)]^-$ (6) and $[\text{TcO}(\text{MAG}_3\text{OMe})]^-$, polymorph 1 (7), are virtually superimposable except for a rotation of the dangling chain about the $\text{N}10-\text{C}11$ axis. The structure of $[\text{TcO}(\text{MAG}_3\text{OMe})]^-$, polymorph 2 (8), differs from $[\text{TcO}(\text{MAG}_3)]^-$ (6) by a rotation in the pendent chain about the $\text{C}11-\text{C}12$ axis. These differences in conformation can be described by the torsion angles $\text{C}9-\text{N}10-\text{C}11-\text{C}12 = 71.8(0.5)^\circ$ in 6, $-116.6(0.4)^\circ$ in 7, and $65.5(0.6)^\circ$ in 8; and $\text{N}10-\text{C}11-\text{C}12-\text{O}12 = -161.2(0.5)^\circ$ in 6, $-151.6(0.5)^\circ$ in 7, and $27.0(0.5)^\circ$ in 8. The bond lengths between the three structures are closely similar. Averaged lengths are $\text{Tc}=\text{O} = 1.653(6)$ Å and $\text{Tc}-\text{S} = 2.286(6)$ Å. The $\text{Tc}-\text{N}$ lengths show small variations according to nitrogen position which may or may not be significant: $\text{Tc}-\text{N}4 = 1.993(8)$ Å, $\text{Tc}-\text{N}7 = 1.973(5)$ Å, and $\text{Tc}-\text{N}10 = 2.02(1)$ Å. Complete details and tabulations for these structures, including the cations, may be found in the supplementary material.

Discussion

The production of $[\text{TcO}(\text{MAG}_3)]^-$ outlined here involves the use of a benzoyl-protecting group on the free sulfur atom of the MAG_3 ligand; this protecting group inhibits oxidation of

the thiol functionality upon long term storage of the radiopharmaceutical kit. The protecting group falls away upon coordination of the ligand to ${}^{99m}\text{Tc}$, providing a clean route to $[\text{TcO}(\text{MAG}_3)]^-$. The manufacture of high purity benzoyl- MAG_3 is crucial to the final purity of the radiopharmaceutical product since radiochemical purities of $>90\%$ are necessary for *in vivo* use. Early reaction schemes for the preparation of benzoyl- MAG_3 gave products which were seriously contaminated, leading to mixtures of ${}^{99m}\text{Tc}$ products from the subsequent complexation reaction. These byproducts interfered with effective renal function imaging, and led to some speculation that chromatography was necessary to purify the $[\text{TcO}(\text{MAG}_3)]^-$ imaging agent prior to use.⁸ The optimized preparation for benzoyl- MAG_3 described herein virtually eliminates the ligand-based contaminants in $[\text{TcO}(\text{MAG}_3)]^-$ and allows the generation of a commercial kit which is convenient for routine hospital use and which eliminates the need for purification of the final radiopharmaceutical. This revised ligand preparation makes use of an activated ester of *S*-benzoylmercaptoacetic acid and has been described independently by Brandau.⁸

Our goal in this present work was to identify the chemical nature of $[\text{TcO}(\text{MAG}_3)]^-$ and to characterize the side products that may be generated during its synthesis. Knowledge of the identity of the undesirable radioactive byproducts is necessary to formulate an efficacious commercial agent. Such knowledge also furthers our understanding of the chemistry and reactions of technetium. Our investigation of the ${}^{99m}\text{Tc}$ products employed the ${}^{99g}\text{Tc}$ analogs. A new reaction scheme was necessary to prepare bulk amounts of $[\text{TcO}(\text{MAG}_3)]^-$ since the preparative method used for $[\text{TcO}(\text{MAG}_3)]^-$ gave unacceptable yields when the mass of technetium was increased.

Table 2. Fractional Atomic Coordinates for [AsPh₄][^{99g}TcO(MAG₃)]

	x	y	z	$U_{eq},^a \text{Å}^2$
Tc	0.4098(1)	0.1024(1)	0.1481(1)	0.029(1)
O1	0.3025(2)	0.1734(3)	0.1185(1)	0.045(1)
S1	0.3663(1)	0.0223(1)	0.2312(1)	0.052(1)
C2	0.3221(4)	-0.1416(5)	0.2112(2)	0.055(2)
C3	0.3705(4)	-0.1843(4)	0.1590(2)	0.039(2)
O3	0.3691(3)	-0.2993(3)	0.1437(2)	0.058(2)
N4	0.4129(3)	-0.0870(4)	0.1288(2)	0.034(1)
C5	0.4723(4)	-0.1214(4)	0.0805(2)	0.040(2)
C6	0.5534(4)	-0.0115(5)	0.0699(2)	0.038(2)
O6	0.6250(3)	-0.0222(3)	0.0374(1)	0.053(1)
N7	0.5363(3)	0.0951(4)	0.1007(2)	0.033(1)
C8	0.6147(4)	0.2020(5)	0.1036(2)	0.039(2)
C9	0.5951(4)	0.2783(5)	0.1547(2)	0.041(2)
O9	0.6536(3)	0.3718(4)	0.1683(2)	0.067(2)
N10	0.5098(3)	0.2353(4)	0.1836(2)	0.035(1)
C11	0.4965(4)	0.3039(5)	0.2346(2)	0.044(2)
C12	0.4551(4)	0.4426(5)	0.2293(2)	0.043(2)
O13	0.4050(3)	0.4662(3)	0.1826(2)	0.054(1)
O12	0.4643(3)	0.5223(4)	0.2648(2)	0.074(2)
As	-0.1185(1)	0.6578(1)	0.0904(1)	0.030(1)
C110	-0.2194(3)	0.5950(5)	0.0360(2)	0.029(2)
C120	-0.2995(4)	0.6803(5)	0.0170(2)	0.042(2)
C130	-0.3753(4)	0.6364(5)	-0.0216(2)	0.052(2)
C140	-0.3718(4)	0.5089(6)	-0.0410(2)	0.055(2)
C150	-0.2911(4)	0.4262(5)	-0.0223(2)	0.051(2)
C160	-0.2149(4)	0.4674(5)	0.0168(2)	0.040(2)
C21	-0.2024(4)	0.7504(5)	0.1416(2)	0.034(2)
C22	-0.1896(4)	0.8840(5)	0.1500(2)	0.043(2)
C23	-0.2554(4)	0.9483(5)	0.1857(2)	0.050(2)
C24	-0.3327(4)	0.8811(6)	0.2126(2)	0.056(2)
C25	-0.3457(4)	0.7492(6)	0.2043(3)	0.066(3)
C26	-0.2806(4)	0.6819(5)	0.1700(2)	0.053(2)
C31	-0.0392(4)	0.5103(4)	0.1193(2)	0.033(2)
C32	-0.0957(4)	0.4058(5)	0.1416(2)	0.043(2)
C33	-0.0376(4)	0.2951(5)	0.1586(2)	0.050(2)
C34	0.0748(4)	0.2885(5)	0.1523(2)	0.047(2)
C35	0.1287(4)	0.3931(5)	0.1310(2)	0.047(2)
C36	0.0732(4)	0.5056(5)	0.1143(2)	0.041(2)
C41	-0.0145(4)	0.7736(4)	0.0594(2)	0.036(2)
C42	-0.0067(4)	0.7802(5)	0.0038(2)	0.045(2)
C43	0.0754(5)	0.8569(5)	-0.0165(2)	0.063(2)
C44	0.1469(4)	0.9253(5)	0.0172(3)	0.068(3)
C45	0.1366(4)	0.9197(5)	0.0728(3)	0.068(3)
C46	0.0561(4)	0.8432(5)	0.0946(2)	0.049(2)

^a U_{eq} is defined as one-third the trace of the orthogonalized U_{ij} tensor.

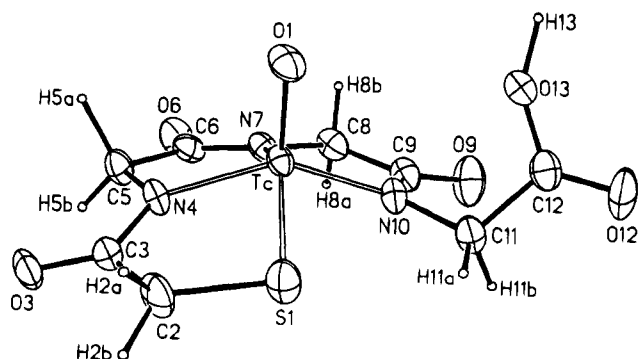


Figure 4. Diagram of the structure of [^{99g}TcO(MAG₃)]⁻, showing the geometry and atomic labeling scheme. Ellipsoids represent 50% probability.

The reaction of deprotected MAG₃ ligand with [^{99g}TcOCl₄]⁻ gave the best results, although significant amounts of side products were generated. This proved fortuitous, since some of these ^{99g}Tc side products were shown to be the same as those generated, to a much lesser extent, in early radiopharmaceutical preparations of [^{99m}TcO(MAG₃)]⁻. The lipophilic impurity

Table 3. Fractional Atomic Coordinates for [PPh₄][^{99g}TcO(MAG₃OMe)]·2H₂O (Polymorph 1)

	x	y	z	$U_{eq},^a \text{Å}^2$
Tc	0.2018(1)	0.0366(1)	0.0705(1)	0.042(1)
O1	0.0536(2)	-0.0084(2)	0.0970(2)	0.059(1)
S1	0.2489(1)	0.2074(1)	-0.0711(1)	0.061(1)
C2	0.2959(4)	0.1535(4)	-0.1795(3)	0.070(2)
C3	0.3388(3)	0.0336(3)	-0.1415(3)	0.058(2)
O3	0.3965(2)	-0.0090(2)	-0.2053(2)	0.071(1)
N4	0.3098(3)	-0.0213(2)	-0.0348(2)	0.054(1)
C5	0.3659(3)	-0.1295(3)	0.0093(3)	0.055(2)
C6	0.3640(3)	-0.1496(3)	0.1252(3)	0.052(2)
O6	0.4185(2)	-0.2260(2)	0.1783(2)	0.065(1)
N7	0.2985(2)	-0.0721(2)	0.1593(2)	0.046(1)
C8	0.3004(3)	-0.0669(3)	0.2623(3)	0.049(2)
C9	0.2570(3)	0.0470(3)	0.2615(3)	0.045(1)
O9	0.2546(2)	0.0761(2)	0.3396(2)	0.063(1)
N10	0.2218(2)	0.1121(2)	0.1737(2)	0.047(1)
C11	0.1902(3)	0.2289(3)	0.1636(3)	0.057(2)
C12	0.0577(4)	0.2522(4)	0.1613(3)	0.060(2)
O12	0.0290(3)	0.3453(3)	0.1158(3)	0.120(2)
O13	-0.0223(2)	0.1628(2)	0.2151(2)	0.072(1)
C14	-0.1515(4)	0.1767(5)	0.2139(4)	0.107(3)
P	0.2533(1)	0.4484(1)	0.3636(1)	0.041(1)
C1A	0.1732(3)	0.5531(3)	0.2793(3)	0.044(1)
C2A	0.1223(3)	0.6429(3)	0.3075(3)	0.050(2)
C3A	0.0584(3)	0.7202(3)	0.2419(3)	0.062(2)
C4A	0.0444(3)	0.7091(3)	0.1497(3)	0.070(2)
C5A	0.0926(4)	0.6185(3)	0.1225(3)	0.071(2)
C6A	0.1583(4)	0.5410(3)	0.1862(3)	0.060(2)
C1B	0.3896(3)	0.4192(3)	0.2773(3)	0.043(1)
C2B	0.4647(4)	0.5111(3)	0.1961(3)	0.061(2)
C3B	0.5677(4)	0.4897(4)	0.1269(3)	0.080(2)
C4B	0.5929(4)	0.3785(4)	0.1367(3)	0.073(2)
C5B	0.5198(3)	0.2883(3)	0.2175(3)	0.063(2)
C6B	0.4173(3)	0.3074(3)	0.2890(3)	0.049(2)
C1C	0.1524(3)	0.3201(3)	0.4368(3)	0.046(2)
C2C	0.1922(3)	0.2304(3)	0.5147(3)	0.060(2)
C3C	0.1165(4)	0.1296(3)	0.5683(3)	0.078(2)
C4C	0.0049(4)	0.1181(4)	0.5445(4)	0.084(2)
C5C	-0.0346(4)	0.2069(4)	0.4684(4)	0.080(2)
C6C	0.0378(3)	0.3091(3)	0.4142(3)	0.059(2)
C1D	0.2914(3)	0.5033(3)	0.4571(3)	0.044(1)
C2D	0.3834(4)	0.5913(3)	0.4210(3)	0.060(2)
C3D	0.4062(4)	0.6397(3)	0.4915(3)	0.072(2)
C4D	0.3395(4)	0.5997(4)	0.5959(4)	0.075(2)
C5D	0.2501(4)	0.5116(4)	0.6330(3)	0.083(2)
C6D	0.2242(3)	0.4630(3)	0.5638(3)	0.063(2)
OW1	0.5683(2)	0.9014(2)	0.4230(2)	0.070(1)
OW2	0.6741(2)	0.0653(2)	0.4807(2)	0.072(1)

^a U_{eq} is defined as one-third the trace of the orthogonalized U_{ij} tensor.

(peak 5 in Figure 1) is positively identified as [^{99g}TcO(MAG₃OMe)]⁻. Another impurity is observed as peak 4 in Figure 1 and is analogous to peak B of Figure 2 in the ^{99m}Tc prep. The behavior of this peak under various HPLC conditions (e.g., ion-pairing mode vs standard reverse phase) leads to the hypothesis that it is more negatively charged and more hydrophilic than [^{99g}TcO(MAG₃)]⁻ and that it converts to [^{99g}TcO(MAG₃)]⁻ with time. Noll and co-workers¹² have recently published a manuscript in which reactions of ^{99m}Tc and ^{99g}Tc with free MAG₃ are described. They conclude that the good donor characteristics of the unprotected mercapto group initially leads to multiple MAG₃ ligands being bound to Tc, and that this purported [TcO(MAG₃)_x]ⁿ⁻ complex is an intermediate which decomposes to [TcO(MAG₃)]⁻ on the time scale of minutes. It is reasonable to suppose that this material might also be an important impurity in our [^{99g}TcO(MAG₃)]⁻ preparation, so that the identity of peak 4 in Figure 1 is tentatively assigned to be [^{99g}TcO(MAG₃)_x]ⁿ⁻.

(12) Noll, B.; Johansen, B.; May, K.; Spies, H. *Appl. Radiat. Isot.* **1992**, *43*, 899–901.

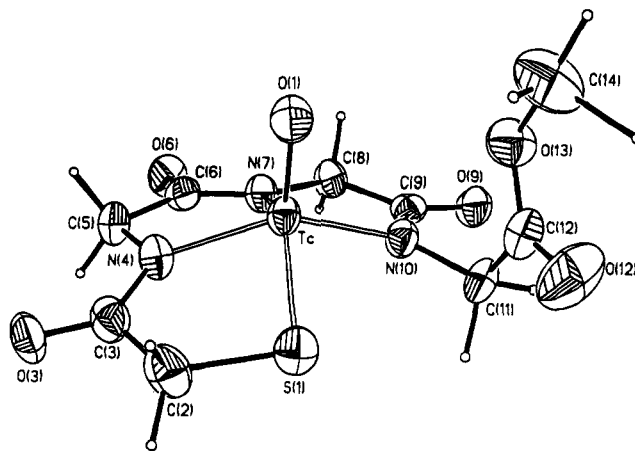
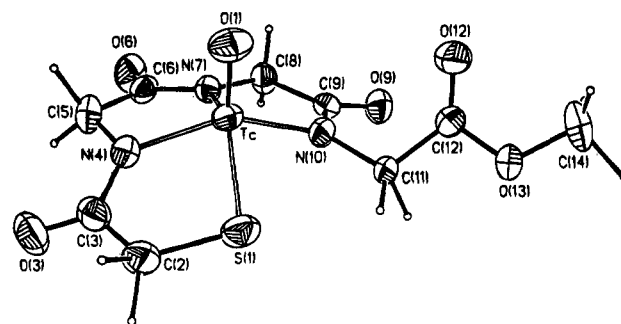
Table 4. Fractional Atomic Coordinates for $[\text{PPh}_4][^{99\text{g}}\text{TcO}(\text{MAG}_3\text{OMe})]\cdot 2\text{H}_2\text{O}$ (Polymorph 2)

	x	y	z	$U_{\text{eq}},^a \text{\AA}^2$
Tc	0.6521(1)	0.7460(1)	0.8584(1)	0.046(1)
O1	0.5907(3)	0.6085(3)	0.7375(3)	0.070(2)
S1	0.5353(1)	0.8174(1)	0.9640(1)	0.069(1)
C2	0.5965(5)	0.7789(5)	1.0880(5)	0.075(4)
C3	0.7168(5)	0.7585(4)	1.1090(5)	0.065(3)
O3	0.7814(4)	0.7569(3)	1.2046(3)	0.087(3)
N4	0.7484(3)	0.7391(3)	1.0138(4)	0.053(2)
C5	0.8684(4)	0.7302(4)	1.0316(5)	0.062(3)
C6	0.9034(5)	0.7881(4)	0.9668(4)	0.053(3)
O6	1.0050(3)	0.8182(3)	0.9878(3)	0.073(3)
N7	0.8107(3)	0.8037(3)	0.8855(3)	0.044(2)
C8	0.8276(4)	0.8746(4)	0.8294(4)	0.050(3)
C9	0.7138(4)	0.9119(4)	0.7852(4)	0.049(3)
O9	0.7046(3)	0.9798(3)	0.7402(3)	0.066(2)
N10	0.6261(3)	0.8694(3)	0.8013(4)	0.051(2)
C11	0.5245(5)	0.9213(5)	0.7747(5)	0.065(3)
C12	0.4641(4)	0.8892(5)	0.6380(5)	0.054(3)
O12	0.4626(3)	0.8021(4)	0.5466(4)	0.084(3)
O13	0.4066(3)	0.9760(3)	0.6325(3)	0.071(2)
C14	0.3376(6)	0.9607(6)	0.5092(6)	0.097(5)
P	-0.1700(1)	0.4153(1)	0.2164(1)	0.040(1)
C1A	-0.2158(4)	0.5340(4)	0.3232(4)	0.040(3)
C2A	-0.3260(4)	0.5109(4)	0.3187(4)	0.048(3)
C3A	-0.3655(4)	0.6012(4)	0.3974(4)	0.055(3)
C4A	-0.2944(5)	0.7150(4)	0.4784(4)	0.059(3)
C5A	-0.1857(5)	0.7386(4)	0.4836(5)	0.062(3)
C6A	-0.1441(4)	0.6475(4)	0.4065(4)	0.051(3)
C1B	-0.0236(4)	0.4676(4)	0.2469(4)	0.040(3)
C2B	0.0702(4)	0.4367(4)	0.3159(4)	0.046(3)
C3B	0.1825(4)	0.4826(5)	0.3431(5)	0.058(3)
C4B	0.2008(5)	0.5606(5)	0.3023(6)	0.069(4)
C5B	0.1083(5)	0.5920(5)	0.2343(6)	0.078(4)
C6B	-0.0041(5)	0.5458(5)	0.2059(5)	0.063(4)
C1C	-0.1739(4)	0.2889(4)	0.2433(4)	0.041(3)
C2C	-0.1862(5)	0.3020(5)	0.3479(5)	0.069(4)
C3C	-0.1808(6)	0.2078(6)	0.3731(5)	0.077(4)
C4C	-0.1657(5)	0.1031(5)	0.2955(6)	0.072(4)
C5C	-0.1491(8)	0.0893(5)	0.1942(7)	0.135(6)
C6C	-0.1523(8)	0.1839(5)	0.1696(6)	0.122(6)
C1D	-0.2623(4)	0.3780(4)	0.0566(4)	0.042(3)
C2D	-0.2649(6)	0.2755(5)	-0.0445(5)	0.087(4)
C3D	-0.3330(6)	0.2509(5)	-0.1674(5)	0.085(4)
C4D	-0.3940(4)	0.3315(4)	-0.1876(4)	0.057(3)
C5D	-0.3900(5)	0.4361(4)	-0.0878(5)	0.068(4)
C6D	-0.3250(5)	0.4603(4)	0.0358(4)	0.061(3)
OW1	-0.0096(4)	0.1111(4)	0.5906(4)	0.114(3)
OW2	-0.1125(5)	0.0869(6)	0.7398(5)	0.200(6)

^a U_{eq} is defined as one-third the trace of the orthogonalized U_{ij} tensor.

The characterized products of the $[\text{PPh}_4][^{99\text{g}}\text{TcO}(\text{MAG}_3)]^-$ preparative reaction can be used to characterize the products of the $[\text{PPh}_4][^{99\text{m}}\text{TcO}(\text{MAG}_3)]^-$ preparative reaction. HPLC co-elution of $[\text{PPh}_4][^{99\text{g}}\text{TcO}(\text{MAG}_3)]^-$ and $[\text{PPh}_4][^{99\text{m}}\text{TcO}(\text{MAG}_3)]^-$ confirms their identical chemical structures. The lipophilic impurity is $[\text{PPh}_4][^{99\text{m}}\text{TcO}(\text{MAG}_3\text{OMe})]^-$, wherein the esterified ligand derives from the reaction of methanol and the carboxylate function of the MAG_3 ligand in base. As a check, the methyl ester complex $[\text{PPh}_4][^{99\text{m}}\text{TcO}(\text{MAG}_3\text{OMe})]^-$ was deliberately synthesized from benzoyl- MAG_3OMe using the same conditions as used during the preparation of $[\text{PPh}_4][^{99\text{m}}\text{TcO}(\text{MAG}_3)]^-$; HPLC confirms the identity of the product by comparison to characterized $[\text{PPh}_4][^{99\text{g}}\text{TcO}(\text{MAG}_3\text{OMe})]^-$.

The structural characterizations of $[\text{PPh}_4][^{99\text{g}}\text{TcO}(\text{MAG}_3)]^-$ and $[\text{PPh}_4][^{99\text{g}}\text{TcO}(\text{MAG}_3\text{OMe})]^-$ contained herein are valuable adjuncts to the elucidation of general $^{99\text{m}}\text{Tc}$ properties. The complexes $[\text{PPh}_4][^{99\text{g}}\text{TcO}(\text{MAG}_3)]^-$ and $[\text{PPh}_4][^{99\text{g}}\text{TcO}(\text{MAG}_3\text{OMe})]^-$ are members of the important class of $\text{Tc}(\text{V})$ complexes which contain a $(\text{Tc}^{\text{V}}=\text{O})^{3+}$ core and a tetradentate chelating ligand. Along these lines, tetradentate- N_2S_2 donor ligands have been the most

**Figure 5.** Diagram of the structure of $[\text{PPh}_4][^{99\text{g}}\text{TcO}(\text{MAG}_3\text{OMe})]^-$ designated as polymorph 1, showing the geometry and atomic labeling scheme. Ellipsoids represent 50% probability.**Figure 6.** Diagram of the structure of $[\text{PPh}_4][^{99\text{g}}\text{TcO}(\text{MAG}_3\text{OMe})]^-$ designated as polymorph 2, showing the geometry and atomic labeling scheme. Ellipsoids represent 50% probability.**Table 5.** Selected Bond Lengths (\AA) in the Anions $[\text{PPh}_4][^{99\text{m}}\text{TcO}(\text{MAG}_3)]^-$ (6), $[\text{PPh}_4][^{99\text{g}}\text{TcO}(\text{MAG}_3\text{OMe})]^-$ (7), and $[\text{PPh}_4][^{99\text{g}}\text{TcO}(\text{MAG}_3\text{OMe})]^-$ (Polymorph 2) (8)

	6	7	8
Tc-O1	1.647(3)	1.654(2)	1.658(3)
Tc-S1	2.279(2)	2.287(1)	2.291(2)
Tc-N4	1.985(4)	1.994(3)	2.000(4)
Tc-N7	1.973(4)	1.969(3)	1.978(4)
Tc-N10	2.003(4)	2.030(3)	2.028(5)
S1-C2	1.815(5)	1.822(5)	1.821(8)
C2-C3	1.497(7)	1.515(6)	1.489(9)
C3-N4	1.350(6)	1.342(4)	1.360(9)
N4-C5	1.458(6)	1.468(4)	1.459(7)
C5-C6	1.524(7)	1.522(6)	1.524(10)
C6-N7	1.342(6)	1.356(5)	1.357(7)
N7-C8	1.451(6)	1.452(5)	1.464(9)
C8-C9	1.503(7)	1.499(5)	1.513(7)
C9-N10	1.356(6)	1.336(4)	1.355(8)
N10-C11	1.451(6)	1.468(5)	1.454(7)

extensively investigated (as potential renal radioimagers,^{13,14} and as potential myocardial¹⁵ and brain perfusion imaging agents¹⁶). Structural data for $(\text{Tc}^{\text{V}}=\text{O})^{3+}$ and $(\text{Re}^{\text{V}}=\text{O})^{3+}$ complexes with N_2S_2 chelates have been recently summarized,¹⁷ yielding the following ranges for structural parameters: $\text{Tc}=\text{O} = 1.65-$

- (13) Davison, A.; Jones, A. G.; Orvig, C.; Sohn, M. *Inorg. Chem.* **1981**, *20*, 1629-1632.
- (14) Fritzbeg, A. R.; Klingensmith, W. C.; Whitney, W. P.; Kuni, C. C. *J. Nucl. Med.* **1981**, *22*, 258-263.
- (15) Ohmono, Y.; Francesconi, L.; Kung, M.-P.; Kung, H. F. *J. Med. Chem.* **1992**, *35*, 157-162.
- (16) Kung, H. F.; Guo, Y.-Z.; Yu, C.-C.; Billings, J.; Subramanyam, V.; Calabrese, J. C. *J. Med. Chem.* **1989**, *32*, 433-437.
- (17) Chen, B.; Heeg, M. J.; Deutsch, E. *Inorg. Chem.* **1992**, *31*, 4683-4690.

Table 6. Selected Bond Angles (deg) in the Anions $[\text{}^{99g}\text{TcO}(\text{MAG}_3)]^-$ (6), $[\text{}^{99g}\text{TcO}(\text{MAG}_3\text{OMe})]^-$ (7), and $[\text{}^{99g}\text{TcO}(\text{MAG}_3\text{OMe})]^-$ (Polymorph 2) (8)

	6	7	8
O1–Tc–S1	110.2(1)	111.1(1)	110.7(2)
O1–Tc–N4	110.0(2)	111.1(1)	109.9(2)
S1–Tc–N4	82.8(1)	82.6(1)	82.5(1)
O1–Tc–N7	112.7(2)	113.8(1)	113.8(2)
S1–Tc–N7	136.8(1)	134.9(1)	135.3(1)
N4–Tc–N7	78.5(1)	78.0(1)	78.7(2)
O1–Tc–N10	111.3(2)	109.5(1)	111.3(2)
S1–Tc–N10	90.6(1)	91.2(1)	90.0(1)
N4–Tc–N10	137.9(1)	138.4(1)	138.1(1)
N7–Tc–N10	78.5(2)	77.8(1)	78.2(2)
Tc–S1–C2	99.4(2)	98.9(1)	100.3(2)
Tc–N4–C3	124.6(3)	124.8(3)	125.7(4)
Tc–N4–C5	116.2(3)	116.8(2)	114.9(4)
Tc–N7–C6	120.3(3)	121.2(2)	119.4(4)
Tc–N7–C8	118.4(3)	118.7(2)	119.8(3)
Tc–N10–C9	117.5(3)	116.9(3)	117.5(3)
Tc–N10–C11	127.9(3)	124.8(2)	128.9(4)

1.66 Å, Re=O = 1.68 Å, M–S(thiol) = 2.25–2.29 Å, M–N(amide) = 1.98–2.05 Å, S–M–N bite angle (5-membered ring) = 82–83°, and N–M–N bite angle (5-membered ring) = 77–80°. These ranges are in agreement with the structural parameters published herein for $[\text{}^{99g}\text{TcO}(\text{MAG}_3)]^-$ and $[\text{}^{99g}\text{TcO}(\text{MAG}_3\text{OMe})]^-$. Complexes containing N_3S basal donor

(18) PIC represents the triply anionic form of *N*-(2-((2-mercaptoacetyl)-amino)ethyl)-2-pyridinecarboxamide. Bryson, N.; Lister-James, J.; Jones, A. G.; Davis, W. G.; Davison, A. *Inorg. Chem.* **1990**, *29*, 2948–2951.

(19) Rao, T. N.; Adhikesavalu, D.; Camerman, A.; Fritzberg, A. R. *Inorg. Chim. Acta* **1991**, *180*, 63–67.

atoms, such as $[\text{TcO}(\text{PIC})]^{18}$ and $[\text{ReO}(\text{MAG}_3)]^-$ ¹⁹ are closely similar to the $[\text{}^{99g}\text{TcO}(\text{MAG}_3)]^-$ and $[\text{}^{99g}\text{TcO}(\text{MAG}_3\text{OMe})]^-$ complexes and likewise show similar geometries within the above ranges. The crystal structure of $[\text{ReO}(\text{MAG}_3)]^-$ is not isostructural with $[\text{TcO}(\text{MAG}_3)]^-$ but is similar enough that it could be isostructural if it were associated with the same cation. Another related set of complexes is $[\text{Tc/ReO}(\text{MAG}_2)]^-$, where MAG_2 is mercaptoacetyldiglycine²⁰ which provides SNNO donor atoms. The structure of $[\text{TcO}(\text{MAG}_2)]^-$ exhibits Tc–S (2.27 Å) and Tc–N (1.97 Å) distances only slightly shorter than the average for $[\text{}^{99g}\text{TcO}(\text{MAG}_3)]^-$ and otherwise is entirely similar.

Acknowledgment. Thanks to Michael Bushman for preparation of the $[\text{}^{99m}\text{TcO}(\text{MAG}_3)]^-$ samples, and to Dr. M. J. Heeg (Department of Chemistry, Wayne State University) for assistance with the preparation of this manuscript.

Supplementary Material Available: Table A contains experimental crystallographic data for all three structures. Anionic bond lengths and angles are shown comparatively in Tables B and C. Anisotropic thermal parameters, hydrogen parameters and cationic bond lengths and angles are listed for $[\text{AsPh}_4][\text{}^{99g}\text{TcO}(\text{MAG}_3)]$ (Tables D–F), $[\text{PPh}_4][\text{}^{99g}\text{TcO}(\text{MAG}_3\text{OMe})] \cdot 2\text{H}_2\text{O}$, polymorph 1 (Tables G–I), and $[\text{PPh}_4][\text{}^{99g}\text{TcO}(\text{MAG}_3\text{OMe})] \cdot 2\text{H}_2\text{O}$, polymorph 2, (Tables J–L). Figures A and B contain additional HPLC tracings (19 pages). Ordering information is given on any current masthead page.

IC940799D

(20) Johannsen, B.; Noll, B.; Leibnitz, P.; Reck, G.; Noll, S.; Spies, H. *Inorg. Chim. Acta* **1993**, *210*, 209–214.